Theory of Excitonic Spectra and Entanglement Engineering in Dot Molecules

Gabriel Bester,[1] J. Shumway,[1,2] and Alex Zunger[1]

[1]National Renewable Energy Laboratory, Golden, Colorado 80401, USA
[2]Department of Physics and Astronomy, Arizona State University, Tempe, Arizona 85287-1504, USA
(Received 27 August 2003; published 22 July 2004)

We present results of correlated pseudopotential calculations of an exciton in a pair of vertically stacked InGaAs/GaAs dots. Competing effects of strain, geometry, and band mixing lead to many unexpected features missing in contemporary models. The first four excitonic states are all optically active at small interdot separation, due to the broken symmetry of the single-particle states. We quantify the degree of entanglement of the exciton wave functions and show its sensitivity to interdot separation. We suggest ways to spectroscopically identify and maximize the entanglement of exciton states.

The small size of semiconductor quantum dots [1] drives speculations that they may provide a physical representation of a quantum bit (qubit) that supports a superposition of "0" and "1" [2–7]. Some proposed representations of qubits include electron spin states [2] and the presence or absence of an electron, hole, or electron-hole pair (exciton) [8–11]. Registers of qubits might be realized in *coupled quantum dots,* self-assembled by strain-driven islanding of InGaAs on a GaAs substrate [12]. In one possibility, an electron represents qubit A and a hole represents qubit B, and the qubit states are the occupation of either the top (T) or bottom (B) dot [8–11]. This quantum register must store entangled states. Predicting entanglement requires a theory of the electronic structure of the dot molecule, including single-particle and correlation effects. Most modeling of dot molecules has been done in single-band effective-mass approximation [7,13–17]. For two equivalent dots, this treatment leads to single-particle electron and hole orbitals forming bonding and antibonding combinations:

$$|\phi_h^b\rangle = \frac{1}{\sqrt{2}}(|h_\mathrm{T}\rangle + |h_\mathrm{B}\rangle), \quad |\phi_h^a\rangle = \frac{1}{\sqrt{2}}(|h_\mathrm{T}\rangle - |h_\mathrm{B}\rangle),$$
$$|\phi_e^b\rangle = \frac{1}{\sqrt{2}}(|e_\mathrm{T}\rangle + |e_\mathrm{B}\rangle), \quad |\phi_e^a\rangle = \frac{1}{\sqrt{2}}(|e_\mathrm{T}\rangle - |e_\mathrm{B}\rangle), \tag{1}$$

where e_T (e_B) represents an electron in the top (bottom) dot and h_T (h_B) represents a hole in the top (bottom) dot. In this picture, as in an H_2^+ molecule, the single-particle *bonding* state energy $E_e^b(d)$ decreases as the interdot distance d decreases, while the bonding hole state energy $E_h^b(d)$ increases. Simple direct products of single-particle states, e.g., $|\phi_e^b\phi_h^b\rangle = \frac{1}{2}[|e_\mathrm{T}h_\mathrm{T}\rangle + |e_\mathrm{B}h_\mathrm{B}\rangle + |e_\mathrm{T}h_\mathrm{B}\rangle + |e_\mathrm{B}h_\mathrm{T}\rangle]$, are *unentangled.* In contrast, the desirable *maximally entangled Bell* states superpose either exciton or dissociated states, but not both:

$$|a\rangle = \frac{1}{\sqrt{2}}(|e_\mathrm{B}h_\mathrm{B}\rangle + |e_\mathrm{T}h_\mathrm{T}\rangle), \quad \text{exciton, bonding;}$$

$$|b\rangle = \frac{1}{\sqrt{2}}(|e_\mathrm{B}h_\mathrm{T}\rangle + |e_\mathrm{T}h_\mathrm{B}\rangle), \quad \text{dissociated, bonding;}$$

$$|c\rangle = \frac{1}{\sqrt{2}}(|e_\mathrm{B}h_\mathrm{T}\rangle - |e_\mathrm{T}h_\mathrm{B}\rangle), \quad \text{dissociated, antibonding;}$$

$$|d\rangle = \frac{1}{\sqrt{2}}(|e_\mathrm{B}h_\mathrm{B}\rangle - |e_\mathrm{T}h_\mathrm{T}\rangle), \quad \text{exciton, antibonding.} \tag{2}$$

Recent optical experiments on vertically stacked double dots [8,11] claimed to show entangled excitonic states, but the evidence for entanglement is indirect and based on a symmetric model underlying Eq. (1). Unlike simple symmetric molecules like H_2^+, double-dot "molecules" of stacked InGaAs dots are made of $\sim 10^5$ atoms and have complicated interactions such as alloy fluctuations, strain, multiband (e.g., light-heavy hole), intervalley (Γ-X), and spin-orbit couplings not included in the symmetric molecular case. To properly simulate these double dots, we have performed detailed atomistic pseudopotential calculations, including correlation, on a realistic dot molecule. In this Letter we report on new insights into the exciton state: all states are optically active at short distances, entanglement is small except at a critical dot separation d_c at which the low energy exciton is darkened, yielding a spectroscopic signature of entanglement.

To understand previous theoretical treatments of excitons in a dot molecule and to set a reference to which our atomistic results are compared, we describe a generic two-site tight-binding Hamiltonian in the basis of products of the electron and hole single-particle states $|e_\mathrm{T}h_\mathrm{T}\rangle$, $|e_\mathrm{B}h_\mathrm{T}\rangle$, $|e_\mathrm{T}h_\mathrm{B}\rangle$, $|e_\mathrm{B}h_\mathrm{B}\rangle$:

$$H = \begin{pmatrix} E_{eh}^{\mathrm{TT}} & t_e & t_h & 0 \\ t_e & E_{eh}^{\mathrm{BT}} & 0 & t_\mathrm{h} \\ t_h & 0 & E_{eh}^{\mathrm{TB}} & t_\mathrm{e} \\ 0 & t_h & t_e & E_{eh}^{\mathrm{BB}} \end{pmatrix}, \tag{3}$$

$$E_{eh}^{TT} = \varepsilon_e^T - \varepsilon_h^T + U_{eh}^{TT}, \qquad E_{eh}^{BT} = \varepsilon_e^B - \varepsilon_h^T + U_{eh}^{BT},$$
$$E_{eh}^{TB} = \varepsilon_e^T - \varepsilon_h^B + U_{eh}^{TB}, \qquad E_{eh}^{BB} = \varepsilon_e^B - \varepsilon_h^B + U_{eh}^{BB} + \Delta E.$$

Here $\{\varepsilon_e^T, \varepsilon_e^B, \varepsilon_h^T, \varepsilon_h^B\}$ are the electron and hole on-site energies, $\{t_e, t_h\}$ are the tunneling matrix elements, and $\{U_{eh}^{TT}, U_{eh}^{TB}, U_{eh}^{BT}, U_{eh}^{BB}\}$ are the electron-hole Coulomb matrix elements. The extra parameter ΔE will be used later in entropy discussion; initially we set $\Delta E = 0$. A simplification, followed in Refs. [8,10,11], is to set $t_e = t_h = t$, $\varepsilon_e^T = \varepsilon_e^B$, and $\varepsilon_h^T = \varepsilon_h^B$, with intradot Coulomb energy $U_{eh}^{TT} = U_{eh}^{BB} = U$, and neglecting interdot terms. The Hamiltonian of Eq. (3) now yields, in increasing order of energy,

$$|1\rangle = (|a\rangle - \gamma_1|b\rangle)/\sqrt{1 + \gamma_1^2}, \qquad |2\rangle = |c\rangle,$$

$$|3\rangle = |d\rangle, \qquad |4\rangle = (|a\rangle - \gamma_2|b\rangle)/\sqrt{1 + \gamma_2^2},$$

$$\gamma_{1,2} = [U \pm \sqrt{(4t)^2 + U^2}]/4t. \qquad (4)$$

We see that in the simplified model states $|2\rangle$ and $|3\rangle$ are fully entangled Bell states [viz. Eq. (2)] that are spatially antisymmetric (antibonding) and therefore optically dark. In contrast, states $|1\rangle$ and $|4\rangle$ are not fully entangled and have some symmetric (bonding) character making them optically allowed. Assuming that the tunneling integral $t(d)$ decays with interdot separation d, the simple model gives the level order shown in Fig. 1(b). In the simple model, the exciton $|1\rangle$ shifts to the red as d decreases, and the separation of the two bright states $|1\rangle$ and $|4\rangle$ increases as $\Delta E = \sqrt{(4t)^2 + U^2}$. Furthermore, the order of the levels is $|1\rangle = $ bright $\rightarrow |2\rangle = $ dark $\rightarrow |3\rangle = $ dark $\rightarrow |4\rangle = $ bright. This is in apparent agreement with experiments that show the same qualitative behavior [8,10,11], spurring hope that the theoretically predicted high degree of entanglement in this system could be experimentally realized to the benefit of quantum computing.

There are reasons to doubt the simple homonuclear diatomiclike analogue of dot molecules of Eq. (1) and Fig. 1(b). Actual self-assembled quantum dots contain $\sim 10^5$ atoms, while the dots themselves are strained by the host matrix and subjected to random alloy fluctuations. Thus, a "molecule" made of two dots does not necessarily behave like homonuclear H_2, but could behave like a heteronuclear molecule (e.g., HF) since strain and alloy fluctuations distinguish the dots, $\varepsilon^T \neq \varepsilon^B$. Furthermore, the electronic properties of such dots cannot [18] be accurately modeled by simple single-band effective-mass approaches: coupling between a large number of bands alters electron and hole localization, changing the Coulomb matrix elements. Finally, the assumption of equal tunneling for electron and hole, $t_e = t_h$, is questionable given the large mass ratio, $m_e/m_{hh} \approx 1/6$, of electrons and heavy holes in the GaAs barrier between the dots. In fact, we see below that band mixing even changes the *sign* of t_h. Thus, a more complete theoretical treatment is warranted.
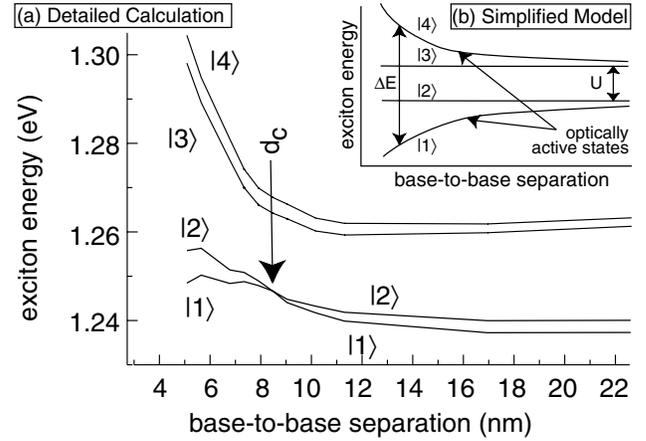
FIG. 1. Exciton energies as a function of the interdot separation for (a) our pseudopotential many-body results. (b) A model calculation $\Delta E = \sqrt{(4t)^2 + U^2}$.

We simulate the InGaAs/GaAs dot molecule at a range of interdot spacings, using a computational approach that successfully describes single InGaAs/GaAs dots [19]. Specifically, we describe the single-particle properties with an atomistic empirical pseudopotential method [20], with the wave functions expanded in a set of Bloch states of the constituent materials over many bands and wave vectors [20]. The theory includes multiband and multivalley coupling, spin-orbit interaction, and anisotropic strain effects. To calculate correlated *e-h* states, we include excitonic effects in a low-order configuration interaction expansion, as in Ref. [21], calculating all Coulomb and exchange integrals explicitly from the single-particle wave functions. The dot geometry has been chosen to resemble the experimental system studied by Bayer *et al.* [8]. As shown in Fig. 2(b), the dots are 12 nm $\times$ 2 nm truncated-cone shaped, with a linear composition gradient varying from $In_{0.5}Ga_{0.5}As$ at their bases to pure InAs at their tops. Figure 3 shows the calculated single-particle energies and wave functions. We plot our calculated correlated *e-h* energies, Fig. 1(a), and corresponding absorption spectra, Fig. 2.

By projecting our numerically calculated correlated *e-h* energies vs d onto a generalized form of H, Eq. (3), we have determined the effective distance-dependent Hamiltonian parameters, shown in Fig. 4. These represent realistic values for the simplified model parameters contemplated in Ref. [2]. Inspection of the parameters from Fig. 4 and the comparison within Fig. 1 show that our results differ in crucial ways from the simple assumptions made in Refs. [8,10,11]. We next discuss the salient features of these differences and their physical implications.

(i) The energies of exciton $|1\rangle$ and $|2\rangle$ blueshift as d decreases, in contrast with the redshift expected from the simple model.—Two effects are responsible for this surprising blueshift. (a) From a *single-particle view,* Fig. 3 shows that as the interdot separation decreases, the energy of both hole states h_0 and h_1 move to lower values, while
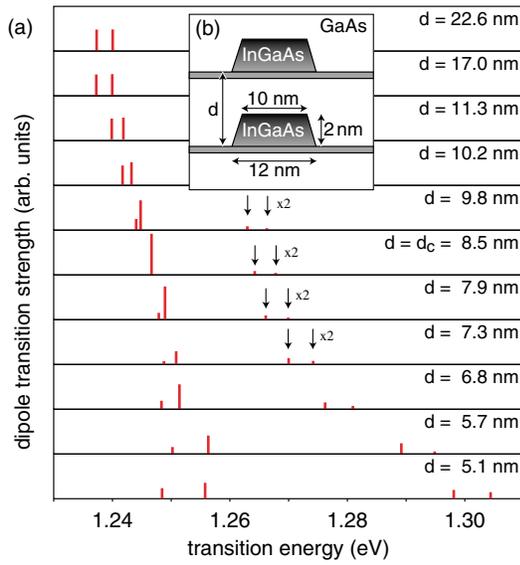
FIG. 2 (color online). (a) Emission spectra in a pair of vertically stacked InGaAs/GaAs dots, calculated with pseudopotential theory. (b) The chosen dot geometry, including a two monolayer (0.56 nm) InGaAs wetting layer and graded composition profile.

the molecular bonding-antibonding picture of Eq. (1) predicts that the bonding h_0 level will move to higher energies. The downward shift of the single-particle hole level h_0 with decreasing d contributes to the upward shift of the lowest excitons $|1\rangle$ and $|2\rangle$ observed in Fig. 1(a). The reason that the single-particle states h_0, h_1 move to lower energies as d decreases is their *symmetry broken* character: h_0 is localized on B and h_1 on T, as seen in the densities, Fig. 3. This localization is reflected in the small tunneling matrix element for holes t_h, in Fig. 4, and is due to the heavier hole mass and the strong strain-induced potential barrier [22] between the dots. In contrast, the light-mass electrons have a large tunneling matrix element t_e and follow the bonding-antibonding picture of Eq. (1), as evidenced by the calculated density, Fig. 3, exhibiting delocalization on both dots. (b) From an *interacting-particle view,* the blueshift of $|1\rangle$ and $|2\rangle$ with decreasing d is caused by the decrease in the Coulomb elements U_{eh}^{TT} and U_{eh}^{BB} with reduced interdot separation [shown in Fig. 4(c)], due to delocalization of the exciton on both dots.

(ii) At large $d > 10$ nm the order of excitons $|1\rangle$, $|2\rangle$, $|3\rangle$, and $|4\rangle$ is bright, bright, dark, and dark, in contrast with the simple model predicting the order bright, dark, dark, bright.—The large d behavior of our pseudopotential calculations can be understood in the tight-binding language: differences in on-site energies $(\varepsilon_e^T - \varepsilon_h^T) - (\varepsilon_e^B - \varepsilon_h^B)$ are greater than hopping elements t_e and t_h (Fig. 4). With these assumptions, the exciton states, in increasing order of energy, are given by $|1\rangle = |e_T h_T\rangle$, $|2\rangle = |e_B h_B\rangle$, $|3\rangle = |e_T h_B\rangle$, $|4\rangle = |e_B h_T\rangle$. States $|1\rangle$ and $|2\rangle$ are bright (the simple model predicts bright and dark, respectively) since they are symmetric and have
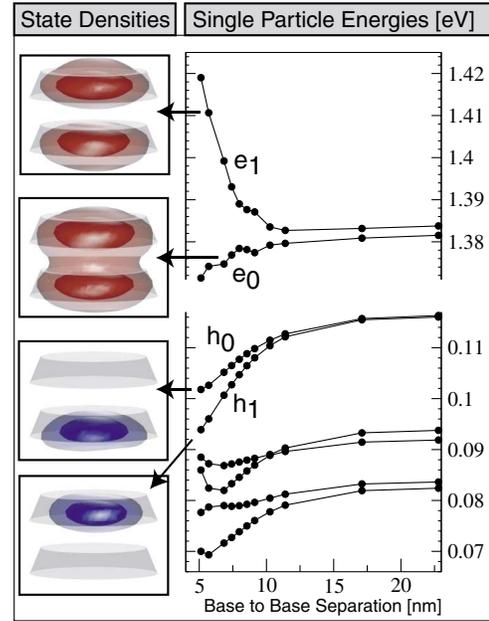
FIG. 3 (color online). Single-particle energies as a function of interdot separation and single-particle state densities from our pseudopotential calculations (for $d = 5.1$ nm). The two translucent isosurfaces enclose 75% and 40% of the total state densities. The physical dot dimensions are shown in gray.

large e-h overlap. In contrast, states $|3\rangle$ and $|4\rangle$ are dark (the simple model predicts dark and bright) since they are not symmetric and have low e-h overlap. These four eigenstates are obviously *not* entangled, while the simple model predicts full entanglement.

(iii) Excitons $|1\rangle$ and $|2\rangle$ anticross at the critical distance d_c at which point $|1\rangle$ becomes dark; however, all excitons are bright at $d < d_c$.—This can be understood as follows. At d_c ($\simeq 8.5$ nm for our specific case) the basis states $|e_T h_T\rangle$ and $|e_B h_B\rangle$ are nearly degenerate. Now hopping elements t_e and t_h split this near degeneracy into
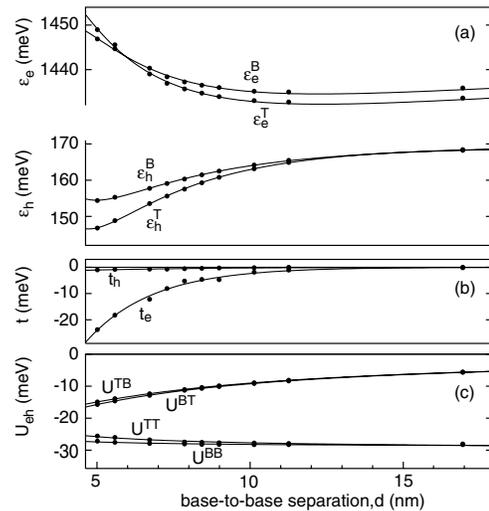
FIG. 4. Effective parameters for the two-site Hamiltonian, Eq. (3), distilled from our pseudopotential calculations.
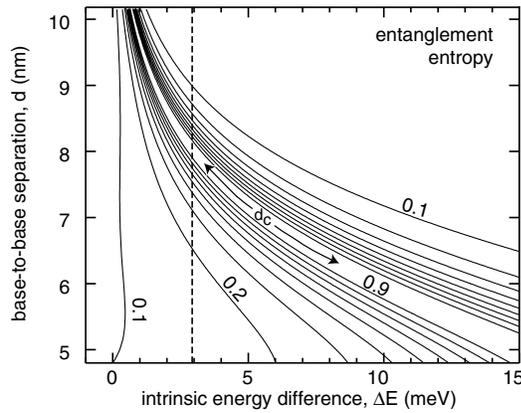
FIG. 5. Degree of entanglement after Eq. (5). The dashed line indicates the value $\Delta E = \varepsilon_e^T - \varepsilon_e^B = 2.9$ meV.

symmetric and antisymmetric combinations $|2\rangle = |a\rangle$ and $|1\rangle = |b\rangle$, respectively. Whether the ground state is symmetric or antisymmetric is decided by the respective signs of t_e and t_h. If they have opposite signs, the symmetric e-h state has lower energy. This is the case in the single band effective mass approximation [16] where the single-particle hole *and* electron states have pure S-envelope-character creating $V_{ss\sigma}$ bonds [23] with positive t_h and negative t_e. However, in a realistic case, the presence of interband mixing [18] (S-P as well as heavy and light-hole) leads to a $V_{pp\sigma}$-like hole bond, with $t_h < 0$. In fact, the confining potential for holes attracts the light-hole P-like component of the hole states to the bonding region between the dots. If t_e and t_h have the same sign [viz. our Fig. 4(b)], the antisymmetric state (dark) is below the symmetric (bright) state.

(iv) The degree of entanglement reaches a maximum at a critical interdot separation d_c.—Since $|1\rangle$ and $|2\rangle$ approach Bell states $|a\rangle$ and $|d\rangle$ at $d = d_c$, we expect high entanglement. We quantify the degree of entanglement versus distance directly from our pseudopotential e-h density matrix, using the von Neumann entropy of entanglement [24],

$$S = -\mathrm{Tr}\, \rho_e \log_2 \rho_e = -\mathrm{Tr}\, \rho_h \log_2 \rho_h, \qquad (5)$$

where ρ_e and ρ_h are the reduced density matrices of the electron and hole, respectively. For exciton $|1\rangle$ we find $S = 0\%$ for $d > 10$ nm and a pronounced peak at d_c with $S = 80\%$. d_c is determined by a balance between interdot strain coupling and intrinsic dot energy differences (alloy fluctuations, in our calculations). To generalize our results to a *class* of dots we allow in Eq. (3) a generic fluctuation, $\Delta E \neq 0$. We have calculated $S(d, \Delta E)$, as shown in Fig. 5, using our fitted model Hamiltonian, Eq. (3) and Fig. 4. This shows how various degrees of entanglement can be engineered. We note that the specific case $d_c = 8.5$ nm arises from our intrinsic dot energy separation $\Delta E = \varepsilon_e^T - \varepsilon_e^B = 2.9$ meV.

Extracting the entanglement from this exciton state for use in quantum computing may require the separation of the electron and hole while maintaining phase coherency. This experimental challenge might be accomplished by driving the particles to nearby dot molecules using an in-plane electric field.

In conclusion, we find that the entanglement entropy reaches a maximum value (of 80% in our case) at a critical interdot separation and decays abruptly to zero at smaller and larger separations. We suggest that the distance d_c can be identified using photoluminescence spectra, by noting two closely spaced exciton peaks with a *darker* lower energy peak.

[1] D. Bimberg, M. Grundman, and N. N. Ledentsov, *Quantum Dots Heterostructures* (John Wiley & Sons, New York, 1999).
[2] D. Loss and D. P. DiVincenzo, Phys. Rev. A **57**, 120 (1998).
[3] P. Zanardi and F. Rossi, Phys. Rev. Lett. **81**, 4752 (1998).
[4] A. Imamoglu *et al.*, Phys. Rev. Lett. **83**, 4204 (1999).
[5] P. Zanardi and F. Rossi, Phys. Rev. B **59**, 8170 (1999).
[6] E. Biolatti, R. C. Iotti, P. Zanardi, and F. Rossi, Phys. Rev. Lett. **85**, 5647 (2000).
[7] F. Troiani, E. Molinari, and U. Hohenester, Phys. Rev. Lett. **90**, 206802 (2003).
[8] M. Bayer *et al.*, Science **291**, 451 (2001).
[9] M. Korkusinski and P. Hawrylak, Phys. Rev. B **63**, 195311 (2001).
[10] M. Korkusinski *et al.*, Physica (Amsterdam) **13E**, 610 (2002).
[11] M. Bayer, Physica (Amsterdam) **12E**, 900 (2002).
[12] I. Shtrichman *et al.*, Phys. Rev. B **65**, 081303 (2002).
[13] L. R. C. Fonseca, J. L. Jimenez, and J. P. Leburton, Phys. Rev. B **58**, 9955 (1998).
[14] C. Yannouleas and U. Landman, Phys. Rev. Lett. **82**, 5325 (1999); **85**, 2220 (2000).
[15] M. Koskinen, S. M. Reimann, and M. Manninen, Phys. Rev. Lett. **90**, 066802 (2003).
[16] F. Troiani, U. Hohenester, and E. Molinari, Phys. Rev. B **65**, 161301 (2002).
[17] T. Fujisawa, D. G. Austing, Y. Tokura, Y. Hirayama, and S. Tarucha, Phys. Rev. Lett. **88**, 236802 (2002).
[18] L.-W. Wang *et al.*, Appl. Phys. Lett. **76**, 339 (2000).
[19] A. J. Williamson, A. Franceschetti, and A. Zunger, Europhys. Lett. **53**, 59 (2001); J. Shumway *et al.*, Phys. Rev. B **64**, 125302 (2001); G. Bester, S. Nair, and A. Zunger, Phys. Rev. B **67**, 161306 (2003).
[20] L.-W. Wang and A. Zunger, Phys. Rev. B **51**, 17 398 (1995); **59**, 15 806 (1999).
[21] A. Franceschetti *et al.*, Phys. Rev. B **60**, 1819 (1999).
[22] W. D. Sheng and J. P. Leburton, Appl. Phys. Lett. **81**, 4449 (2002).
[23] W. A. Harrison, *Electronic Structure and the Properties of Solids* (Freeman San Francisco, San Francisco, 1980).
[24] C. Bennett, H. Bernstein, S. Popescu, and B. Shumacher, Phys. Rev. A **53**, 2046 (1996).